ASCAT Calibration 2010

Doc.No. : EUM/MET/TEN/11/0198
Issue : v2C
Date : 24 March 2011
WBS :

EUMETSAT
Eumetsat-Allee 1, D-64295 Darmstadt, Germany
Tel: +49 6151 807-7
Fax: +49 6151 807 555
http://www.eumetsat.int

Table of Contents

1 INTRODUCTION

The Advanced Scatterometer (ASCAT) on Metop-A is calibrated by means of three transponders based in Turkey. A calibration campaign in November to December 2006 using a single transponder produced a preliminary calibration for ASCAT. The first campaign using all three transponders took place between November 2007 to February 2008 and the resulting calibration (described in [1] and [2]) marked the end of the ASCAT commissioning phase.

A second campaign using three transponders took place between March and July 2010. This document describes

- the data that was acquired,
- the calibration algorithms and procedures that were used,
- the results that were obtained.

A comparison against data from the previous calibration campaign is also presented.

Section 2 describes the data obtained during the campaign and the quality control procedures that were applied. Section 3 gives an overview of the calibration algorithms and software. Section 4 describes modifications to the algorithms (that were made in order to deal with pointing differences between data from ascending and descending passes) and presents the calibration results. A comparison between the results from the 2007 and 2010 calibrations is given in section 5. Ocean and rainforest backscatter is examined in sections 6 and 7 in order to verify the calibration results. Section 8 examines oscillations in the gain pattern. The effect of atmospheric water vapour on the transponder signal is examined in section 9. Finally, section 10 presents conclusions and recommendations.

All input/output data to this transponder calibration campaign has been captured on a CD. It contains

- all L0 input data,
- all transponder logs,
- all ASCA_CAL, ASCA_XCL, ASCA_NTG and L1b files examined during the analysis that lead to this report,
- all off-line code used for AGPO processing.

The PPF being the operational ASCAT L1 processing software is under strict configuration control in OPS. However, for completeness, the versions used have also been included in this CD.

2 TRANSPONDER DATA

The calibration campaign lasted from the 15th of March until the 5th of July 2010 with a total of 139 passes over the transponders. Each transponder produces a number of files for each pass that contain telemetry, pointing information, error messages and captured ASCAT pulse shapes. These files are identified by a number associated with the operation of each transponder. Table 1 shows the transponder operation numbers during the campaign.

transponder	operation number
1	255 - 359
2	197 - 294
3	407 - 506

Table 1. Transponder operations during the 2010 calibration campaign.

Whenever the ASCAT processor detects a transponder signal in the level 0 data, the first step of the calibration procedure is automatically performed and a CAL file containing antenna gain as a function of nominal antenna coordinates is produced.

The procedure used to check the quality of the transponder and CAL data is as follows:

- The logfile is checked to determine if the transponder operation was successful. If so, the remaining data files (apslog, apsvec, housekeeping, status, pulse measurement, and resampled pulse files) are checked to ensure that there are no obvious problems. In particular the status file is examined to determine if the transponder telemetry is within limits, and the apslog and apsvec files are compared to check that the transponder pointing error is small.

- The CAL files are examined to ensure that there are no obvious problems with either the antenna gain values or nominal antenna coordinates.

- The CAL data is cross checked against the transponder data to ensure that there are no missing or extra CAL files.

- The gain values in the set of CAL files are plotted and examined to find outliers.

This process was repeated regularly throughout the campaign and the resulting information was used to schedule ASCAT and transponder operations so that at least two good transponder measurements on every cut through every beam were obtained.

During this campaign:

- There were 5 instances where the tracking error was greater than a threshold of 0.06 degrees. All of these occurred with transponder 1 (operation numbers 258, 291, 306, 322 and 340) and four of these were on the cut with the largest transponder elevation angle.

- There was one occasion where noise in the ASCAT measurement exceeded a 55 dB threshold and was treated as a transponder signal (transponder 2, operation 235). This resulted in unusual values in the CAL file.
- Ten small outliers were found in the CAL gain values. (Transponder 1 operations 255, 334, 261, 317 & 330. Transponder 2 operations 233 & 213. Transponder 3 operations 489, 484 & 468).
- There were a number of occasions when the telemetry was out of limits. However, investigation showed this to be at only a single point during the pass and hence this was not regarded as important.

Figure 1 shows the complete data set. Red and green symbols show the accepted and rejected data. Note that a complete cut has been lost in near range in the left hand beams because of bad tracking by transponder 1.

The campaign was originally scheduled to last for 2 months. However the strategy of examining all data as it arrived, discarding poor quality data and rescheduling transponder operations in order to repeat the pass meant that the campaign actually lasted for 4 months. In particular, there were many attempts to obtain good quality data for near range cut in the left hand beams before accepting that this was not possible due to transponder problems.

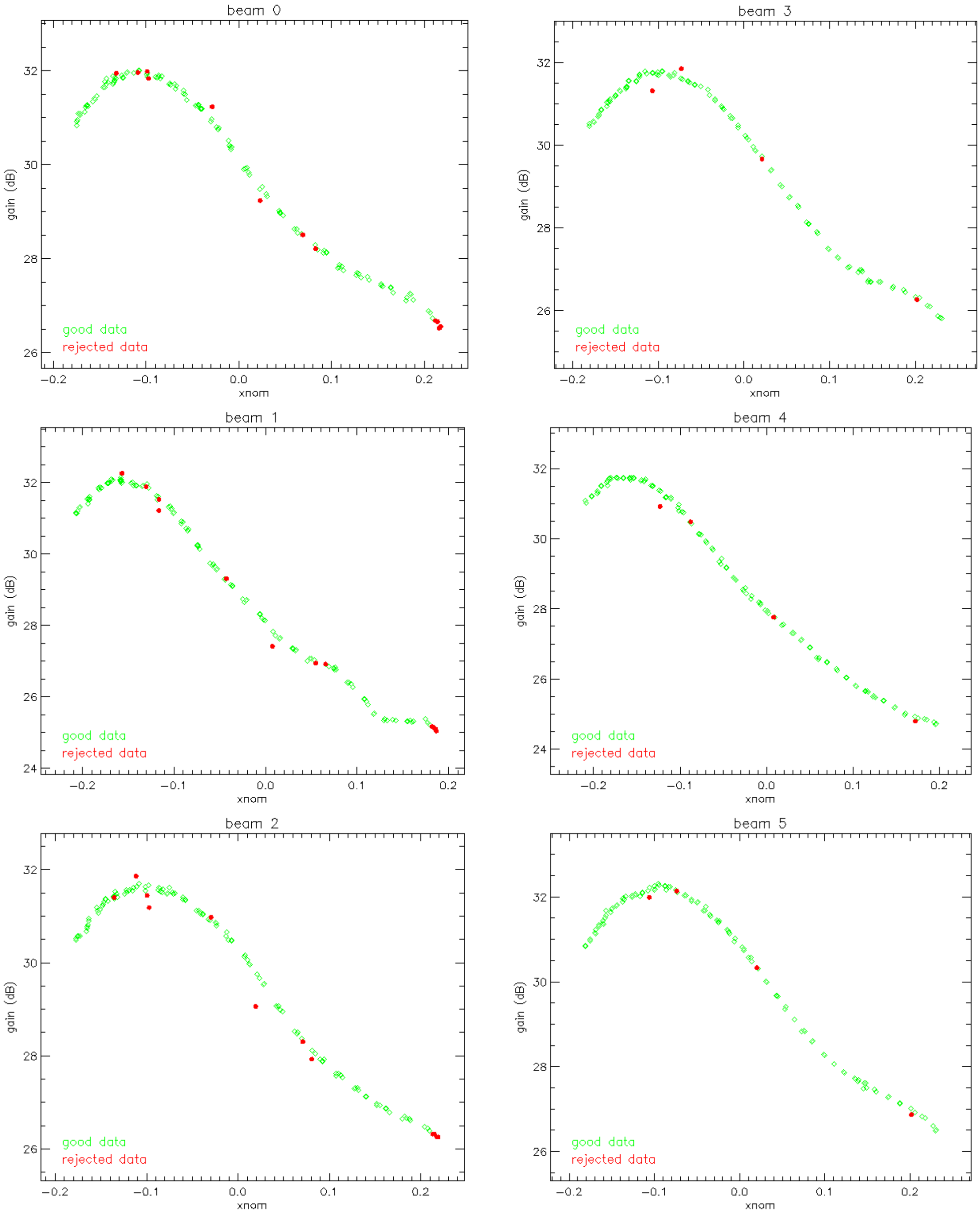

Figure 1. GAPE data from the 2010 calibration campaign.

3 CALIBRATION PROCEDURE

The calibration process consists of three main steps:

- Gain at Angular Position (GAPE) – the signal from each transponder measured by ASCAT is processed to give the antenna gain as a function of the nominal antenna coordinates.
- Antenna Gain Pattern and Orientation (AGPO) – a model of antenna gain and pointing is fitted to a set of GAPE data.
- Normalisation Table Generation (NTG) – the antenna gain model is used to derive tables of normalisation factors that can be used to convert ASCAT measurements into absolutely calibrated backscatter.

An overview of the algorithms and software for each of these steps is given in the following sections.

3.1 GAPE

Whenever the operational processer encounters ASCAT data containing a transponder signal it uses the ASCAT measurement and geolocation information to calculate the antenna gain as function of antenna coordinates and writes these to a CAL file. These files are used for monitoring purposes during the campaign. After completion of the campaign the latest version of the PPF running as a standalone in the TCE is used to reprocess the entire set of calibration data into new CAL files. The offline reprocessing is required as

- the operational processor may occassionally miss a calibration sequence,
- the calibration algorithms are still being developed and modified and the operational processor is usually not the most up to date version,
- the calibration data from previous campaigns must be reprocessed with the same algorithms for comparison purposes and this is simplest to achieve by using a standalone processor.

The standalone PPF was configured as follows:

- s/w: v7.4, which included a fix to correct for AR.11991 as the only change in the GAPE processing w.r.t to the ASCAT PPF version running in the operational ground segment (i.e., v7.3)
- auxiliary files: ASCA_INS_M02_ v2.5 (r64), ASCA_PRC_M02 v5.0 (r71) and ASCA_XTC_xxx v1.7 (r63).

This software for the GAPE procedure has been tested by source code inspection and by comparison against the results from an independent implementation of the algorithms in IDL. The comparison shows that the two sets of results agree to approximately 0.01 dB.

3.2 AGPO

The AGPO algorithm minimises the difference between a model of the antenna gain and the GAPE data by varying the free parameters in the model. This algorithm has been continually modified and improved in order to deal with unexpected properties of the GAPE data.

This calibration step is currently performed by standalone software written in IDL and it is planned to update the operational PPF with the algorithm developed and used during this 2010 calibration campaign.

A description of the latest version of the AGPO algorithm is given in a later section.

3.3 NTG

The normalisation tables were originally calculated by an offline version of the PPF using a single orbit state vector representative of the 29 day orbital cycle of Metop A. In order to deal with orbit eccentricity variations, the speed of the NTG algorithm was increased by removing both the azimuthal and range look averaging. This allowed it to run operationally on an orbit-by-orbit basis so that normalisation tables could be produced for every orbit state vector.

The software for the NTG procedure has been tested by comparing its results against those from an independent implementation of the algorithms in IDL. The two sets of results agree to around 0.01 dB.

The standalone PPF was configured as follows:

- s/w: v7.4, where the NTG is identical to that running in the operational ground segment (i.e., v7.3).
- auxiliary files: ASCA_INS_M02_ v2.5 (r64), ASCA_PRC_M02 v5.0 (r71)
- input ASCA_XCL file as provided by the AGPO algorithm and entered into SVN as v2.2 (r76).

4 MODIFICATIONS TO AGPO

Figure 2 shows the mean γ_0 over Amazon rainforest in the right hand beams for descending passes during 2007 in both SZR (25 km resolution) and SZO (50 km resolution) data. A number of oscillations are seen in the fore beam of the SZR data although these have been mostly smoothed out in the SZO data.

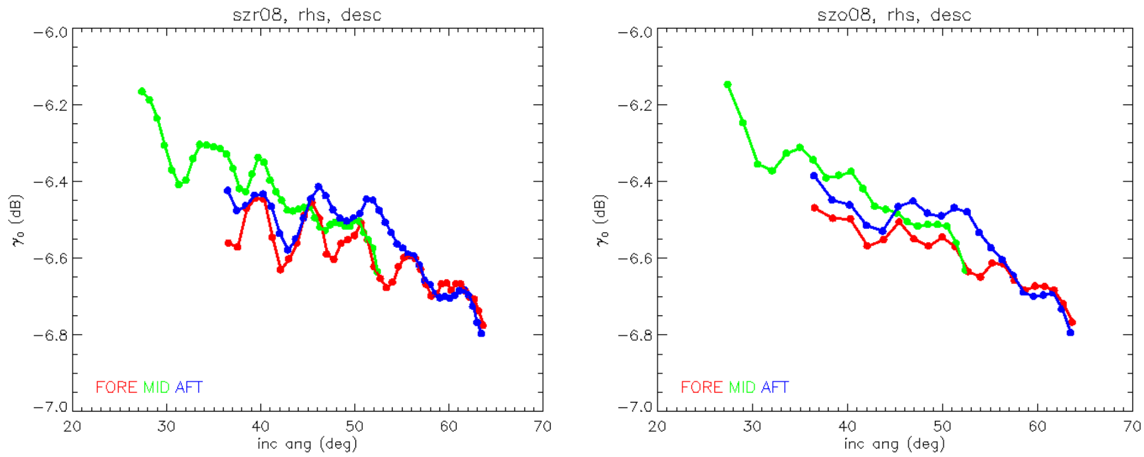

Figure 2. Mean rainforest γ_0 in SZR and SZO data.

Oscillations are also found in the normalization tables and gain patterns. For example figure 3a shows a contour plot of the right fore beam pattern and oscillations towards the edges of the beam can clearly be seen.

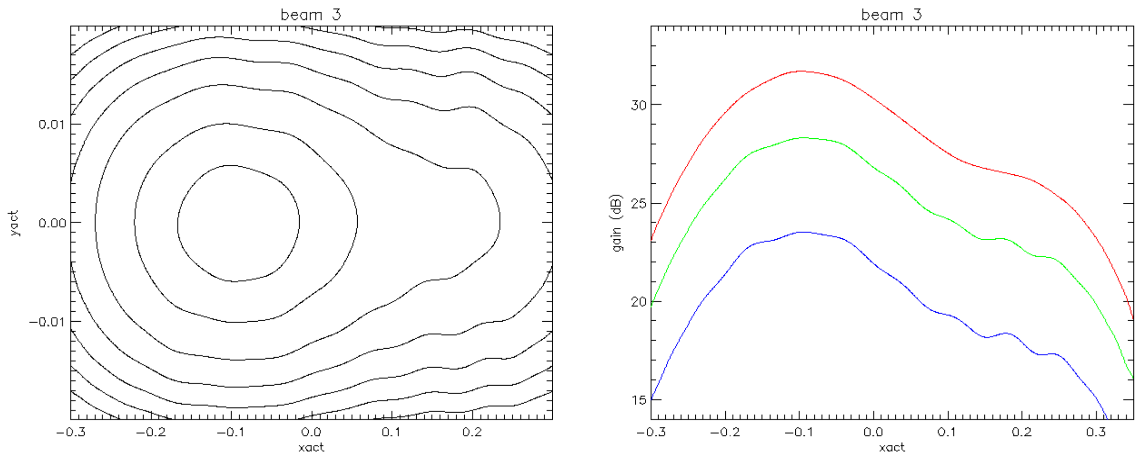

Figure 3. (a) Contour plot of the gain pattern for the right fore beam (b) Three cuts along the elevation axis through the gain pattern.

Figure 3b shows cuts through the gain pattern along the elevation axis at three different values of the azimuthal angle (one corresponding to the centre of the beam, one close to the edge of the beam and a third intermediate value). Although the gain at the centre of the beam (upper red line) is smooth, the gain towards the beam edges contains oscillations.

Examination of data from the transponders shows that the gain values in ascending and descending passes appear to be offset in the azimuth direction. This indicates that the mean pointing for ascending and descending passes is different which may be due to their different mean thermal conditions. The pattern of ascending and descending passes along the elevation axis then gives rise to systematic oscillations in the gain values. As a result of this, the gain pattern model fitted to the data during the AGPO calibration step also contains oscillations and hence gives the behavior seen in figure 3.

In order to solve this problem, the AGPO algorithm has been modified so that the data from each pass is aligned with the nominal gain pattern in order to remove azimuthal depointing effects. The complete AGPO algorithm is described in the following sections and illustrated using data from the left fore beam. Summary results for all beams are presented later.

4.1 Nominal gain model

In the first part of the AGPO algorithm we obtain a nominal gain model by

- calculating weights so that each transponder contributes equally to the data set,
- fitting the gain model to the weighted data by varying three depointing angles, a gain scaling factor, side lobe ratio and phase scaling factor (6 parameters),
- refitting the model by keeping the depointing angles fixed and varying the gain scaling factor, side lobe ratio, the antenna phases and the amplitudes (26 parameters).

The solid black lines in figure 4 shows the resulting nominal gain for three different azimuthal angles (one corresponding to the centre of the beam, one close to the edge of the beam and the third at an intermediate position). The red and green symbols show the ascending and descending pass GAPE data close to these azimuthal angles. We note that the data and model agree well and that at the edge of the beam the model lies midway between the ascending and descending pass data.

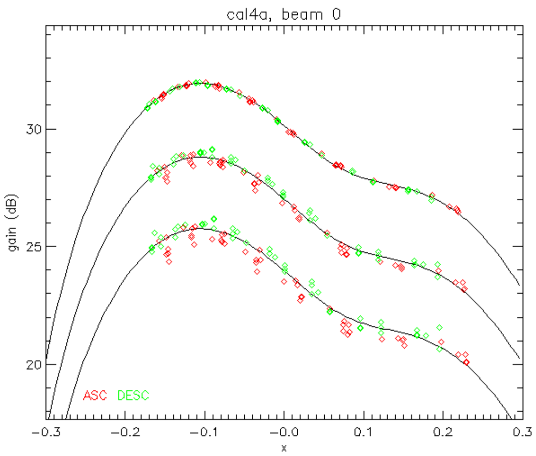

Figure 4. GAPE data and fitted nominal gain model.

4.2 Inter-transponder bias correction

The difference between the nominal gain model and data along the centre of the beam is shown in figure 5. The data from transponder 3 (blue symbols) seems to be biased low while the data from transponder 2 (green symbols) seems to be biased high. Inter-transponder biases are not unexpected per se, but their effect on the measured gain values needs to be corrected before fitting an antenna model.

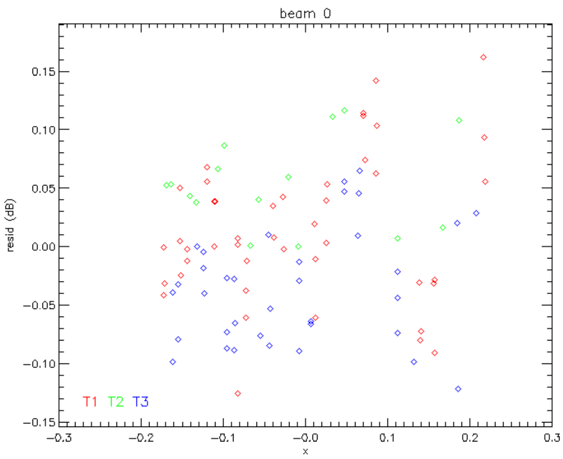

Figure 5. Residuals between data and model along the centre of the beam.

In order to determine the inter-transponder bias we use the following approach:

- Bias values of b_1 and b_2 are subtracted from the data provided by transponders 1 and 2. In order to maintain the mean value of the data, a value of b_1+b_2 is added to the data from transponder 3.
- A gain model is fitted to the bias corrected data along the centre of the beam and the residual is calculated.
- The values of b_1 and b_2 are varied in order to minimise the residual.

The inter-transponder bias values are determined for each beam and an average over all the beams calculated. If the data is now corrected using the mean bias values then the residuals along the centre of the beam, shown in figure 6, now appear to be unbiased and small scale variations (caused by distortions in the antenna gain pattern which not captured by the nominal gain model) can be clearly seen. The resulting residuals refer now all consistently to an average transponder signal, which may be considered as the absolute transponder calibration.

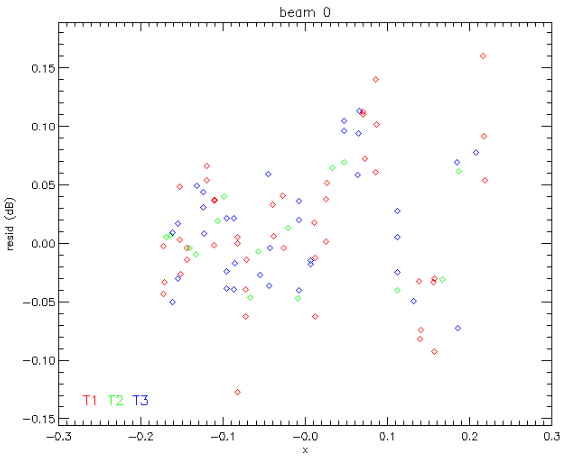

Figure 6. Residuals between bias corrected data and gain model.

4.3 Correction of azimuthal depointing

Differences in the azimuthal pointing can be removed by finding an azimuthal pointing value for each cut that brings the gain values into alignment with the nominal gain model. The corrected data is shown in figure 7 and we see that the ascending and descending pass data (red and green symbols) now agrees well at the edge of the beam as well as along the centre.

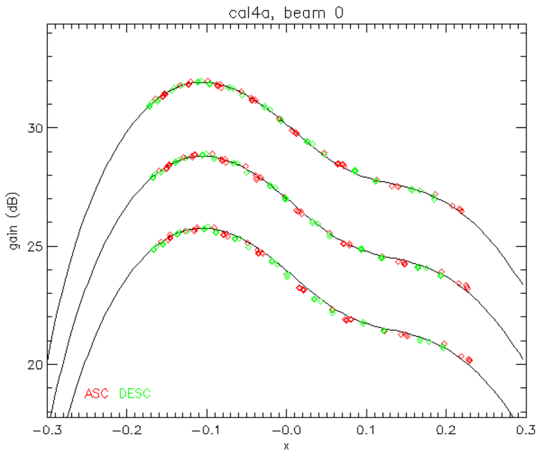

Figure 7. Azimuthally corrected data and gain model.

4.4 Extended data set

The data from the transponders covers only a limited range of incidence and azimuth angles. We require a model that covers a wide range of values and in order to do this we

- extend the data on each cut to higher and lower azimuthal angles by adding additional points whose gain values are given by the nominal gain model,
- extend the data set to higher and lower elevation angles by adding extra cuts whose gain values are given by the fitted nominal gain model.

An example of the extended data set is shown in figure 8.

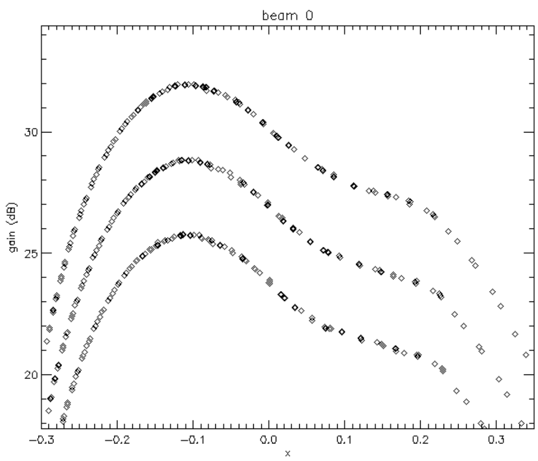

Figure 8. Extended data set obtained using the nominal gain model.

4.5 Distorted gain model

In the final part of the AGPO procedure, we fit a model to the extended data set and then sample it on a grid of azimuthal and elevation angles. This is achieved by looping over the required azimuthal angles and for each of these

- interpolating the data on each cut to obtain a set of gain values and elevation angles,
- fitting a polynomial model to this set of values,
- using the polynomial model to give the gain at the required elevation angles.

The order of the polynomial has to be chosen manually. If it is too low then the model does not accurately fit any small distortions in the beam pattern. If it is too high then the model overfits the data and introduces noise. A polynomial order of around 18 was found to be generally satisfactory and typical results are shown in figure 9.

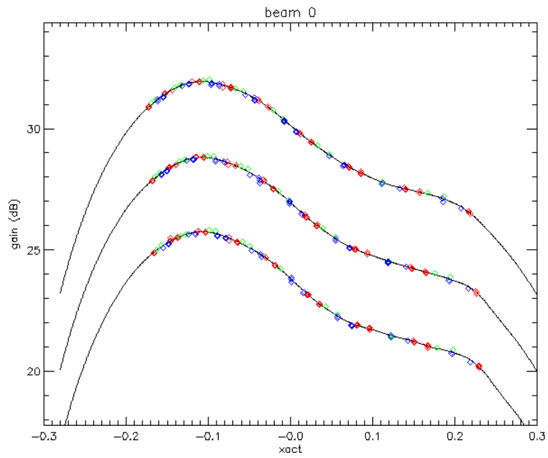

Figure 9. Bias and azimuthally corrected GAPE data and distorted gain model.

The residuals between model and data along the centre of the beam are shown in figure 10. These are small and noiselike with no obvious dependencies on either transponder or elevation angle.

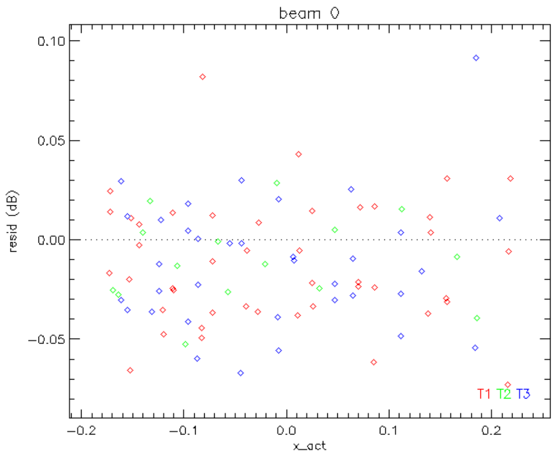

Figure 10. Residual between data and distorted gain model.

The discretely sampled gain model and the three depointing angles are then saved for use in calculation of the normalisation tables.

4.6 Results for all beams

The depointing angles given by fitting the nominal gain model are shown in table 2.

beam	elevation	azimuth	skew
0	-0.0025	0.0013	-0.0021
1	0.0102	0.0006	-0.0008
2	0.0043	-0.0015	0.0016
3	0.0223	0.0015	-0.0010
4	0.0028	-0.0002	0.0008
5	0.0140	-0.0020	0.0020

Table 2. The elevation, azimuth and skew depointing angles (in radians).

The inter-transponder biases in each beam are shown in Table 3. The bias in T1 with respect to the average absolute transponder signal is approximately zero, T2 is biased high and T3 is biased low.

beam	T1	T2	T3
0	0.003	0.020	-0.023
1	-0.010	0.030	-0.019
2	-0.008	0.021	-0.013
3	-0.003	0.032	-0.029
4	-0.008	0.031	-0.023
5	-0.010	0.020	-0.010

Table 3. Inter-transponder bias in each beam (dB).

The average inter-transponder bias given by these figures is shown in table 4 and suggests a difference in calibration levels of about 0.045 dB between transponders 2 and 3.

T1	T2	T3
-0.006	0.026	-0.020

Table 4. Average inter-transponder bias (dB).

Finally, the RMS error between the distorted gain model and the corrected GAPE data is shown in table 5. These values have to be treated with caution as they are, to some extent, a function of the order of the polynomial used to fit the data.

beam	RMSE
0	0.044
1	0.042
2	0.039
3	0.032
4	0.039
5	0.036

Table 5. RMS error (in dB) between the corrected GAPE data and the gain model.

The ASCAT transponder specification is given in [6] and gives a figure of 0.15 dB peak to peak for the stability of the transponder radar cross section. This can be regarded as an error of ±0.075 dB and, as the antenna gain is derived using the square root of the transponder RCS, this implies an error of ±0.037 dB in the antenna gain. This is consistent with the figures given in table 5.

5 COMPARISON

The long term behaviour of the ASCAT can be investigated by comparing the 2010 calibration results against those from 2007. The following sections compare the two using the GAPE data, AGPO results and normalisation tables.

5.1 GAPE

Figure 11 shows the GAPE data from the 2007 campaign in red and the results from the 2010 campaign in green. The two sets of data cannot be directly compared as variations in the satellite orbit mean that the cuts through the gain pattern occur at slightly different elevation angles. However, if we fit a simple model through the 2007 data (shown as a solid line in figure 11) we can then find the difference between this and the 2010 data. The results for beam 0 are shown in figure 12 and the mean difference is 0.053 dB.

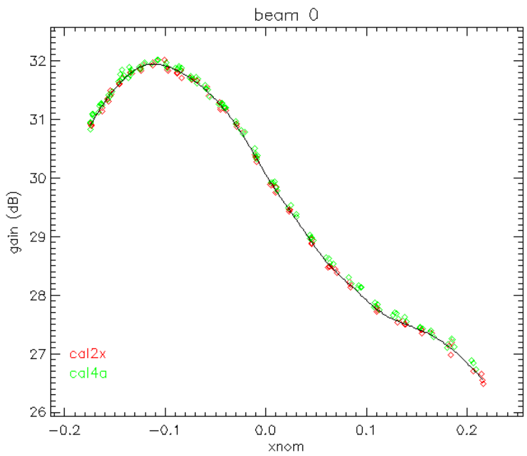

Figure 11. GAPE data from 2007 and 2010 (red and green symbols) and model fitted to 2007 data (solid line)

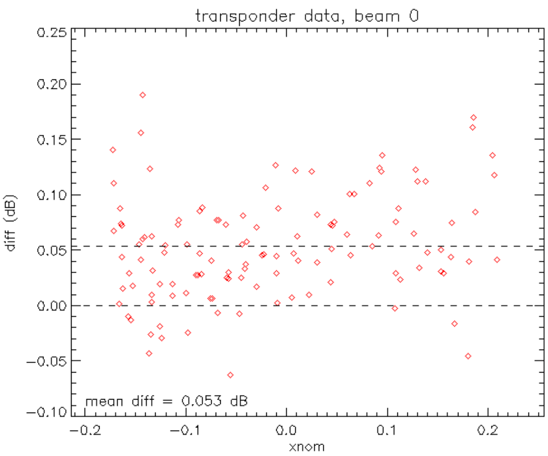

Figure 12. Difference between 2010 data and the 2007 model.

The results for all beams are shown in table 6. Compared to the 2007 data, we find that the gain values in the 2010 campaign have increased by about 0.05 dB in all beams apart from beam 1 where the increase is approximately 0.1 dB. Note that this method comparison is relatively rough and ready as it does not take into account antenna depointing or inter-transponder biases and may also be affected by the method of model fitting.

beam	difference
0	0.053
1	0.110
2	0.069
3	0.049
4	0.040
5	0.050

Table 6. Mean difference (in dB) between 2010 GAPE data and model fitted to 2007 GAPE data, showing an increase between the two campaigns.

These results also allow us to make some preliminary predictions about changes in backscatter. As the normalisation factor is roughly proportional to the two way gain pattern, we can anticipate that the normalisation tables derived from the 2010 data will decrease the backscatter by about 0.2 dB in beam 1 and about 0.1 dB in the other beams.

The data from each transponder can also be investigated using this approach. The results are shown in table 7 and suggest that the gain values measured from transponder 3 have increased by more than those measured from transponders 1 and 2.

beam	T1	T2	T3
0	0.045	0.014	0.069
1	0.089	0.097	0.113
2	0.061	0.044	0.080
3	0.021	0.028	0.076
4	0.013	0.024	0.060
5	0.028	0.035	0.078

Table 7. Mean difference in the gain values measured from each transponder (in dB) given by comparing the 2007 and 2010 GAPE data, showing an increase between the two campaigns..

Taking an average over the beams (but excluding beam 1 as it seems to be behaving in a non-typical fashion) we find that the gain as measured from the transponders 1, 2, and 3 has increased by 0.034, 0.029 and 0.073 dB, respectively.

5.2 AGPO

The data from the 2007 campaign was reprocessed using the same algorithms as the 2010 data. Note that the same quality control procedure could not be used as some of the transponder data from the 2007 campaign did not contain tracking information.

The depointing angles for the 2007 AGPO results are shown in table 8 and we note that they are very similar to those shown in table 2.

beam	elevation	azimuth	skew
0	-0.0015	0.0010	-0.0023
1	0.0114	0.0003	-0.0011
2	0.0054	-0.0018	0.0011
3	0.0189	0.0011	-0.0013
4	0.0022	-0.0003	0.0001
5	0.0107	-0.0023	0.0007

Table 8. Depointing angles in 2007 AGPO results (radians).

The inter-transponder biases, calculated by the same method as described in section 4.2, are shown in table 9. Note that these biases are then with respect to the average absolute transponder signal as measured in the 2007 data.

beam	T1	T2	T3
0	0.002	0.047	-0.049
1	0.010	0.036	-0.046
2	-0.005	0.033	-0.028
3	0.018	0.044	-0.063
4	0.010	0.038	-0.049
5	0.004	0.034	-0.038

Table 9.Inter-transponder bias (dB).

The inter-transponder bias for each transponder found by averaging over all beams is shown in table 10.

T1	T2	T3
0.006	0.039	-0.046

Table 10. Mean inter-transponder bias (in dB).

Comparing these against the figures shown in table 4, we find that the inter-transponder bias of T1 and T2 are approximately unchanged whereas that of T3 has changed by around 0.025 dB.

As a consistency check, we take the bias values of 0.006, 0.039 and -0.046 dB, add the average change for each transponder calculated in the previous section (0.034, 0.029 and 0.073 dB) and we obtain values of 0.040, 0.068 and 0.027 dB. Relative to their mean value of 0.045 dB these become -0.005, 0.023 and -0.018 dB which are essentially the same as the values -0.06, 0.026 and -0.020 given in table 4. This shows that the method for removal of inter-transponder biases is effective and that GAPE and AGPO procedures have been consistently applied to both sets of data.

The RMS difference between the 2007 data and the fitted gain models are shown in table 11. These are similar to the 2010 results.

beam	RMSE
0	0.032
1	0.044
2	0.041
3	0.031
4	0.037
5	0.040

Table 11. RMS error (dB).

The gain patterns produced by the AGPO algorithm can be compared by

1. obtaining a set of gain values at discrete points along the centre of the beam patterns in the actual coordinate system,
2. converting from actual to nominal coordinates,
3. interpolating the two data sets onto a common set of nominal elevation values,
4. calculating the mean difference between the two sets of interpolated gain values.

The results are shown in table 12 and indicate that the antenna gain as estimated from the two different campaigns has changed by about 0.1 dB in beam 1 and about 0.04 dB in the other beams. These values are very similar to those obtained in the previous section from the GAPE data and ensure that no additional effects have been introduced during the AGPO processing, with respect to the direct GAPE measurements comparison.

beam	Mean difference
0	0.039
1	0.098
2	0.056
3	0.035
4	0.032
5	0.041

Table 12. Mean difference between the 2007 and 2010 estimated gain patterns (in dB), showing an increase in gain between the two campaigns.

5.3 NTG

The normalisation tables are used by the level 1b processor to convert the ASCAT measurements into absolutely calibrated backscatter. Any differences between the tables derived from the 2007 and 2010 gain patterns would be expected to be consistent with the differences between the antenna gain patters as estimated from the two campaigns.

Figure 13 shows the difference between the 2007 and 2010 normalisation tables in each beam as a function of node number. The mean difference between them is shown in table 13 and is around 0.2 dB in beam 1 and 0.07–0.11 dB in the other beams. This is approximately twice the mean change in the gain values noted in the previous section, which is as expected since the normalisation factor varies approximately as the square of the gain value.

beam	mean difference
0	0.081
1	0.201
2	0.113
3	0.075
4	0.070
5	0.074

Table 13. Mean difference between 2007 and 2010 normalisation tables (in dB), showing consistently an increase between the two campaigns.

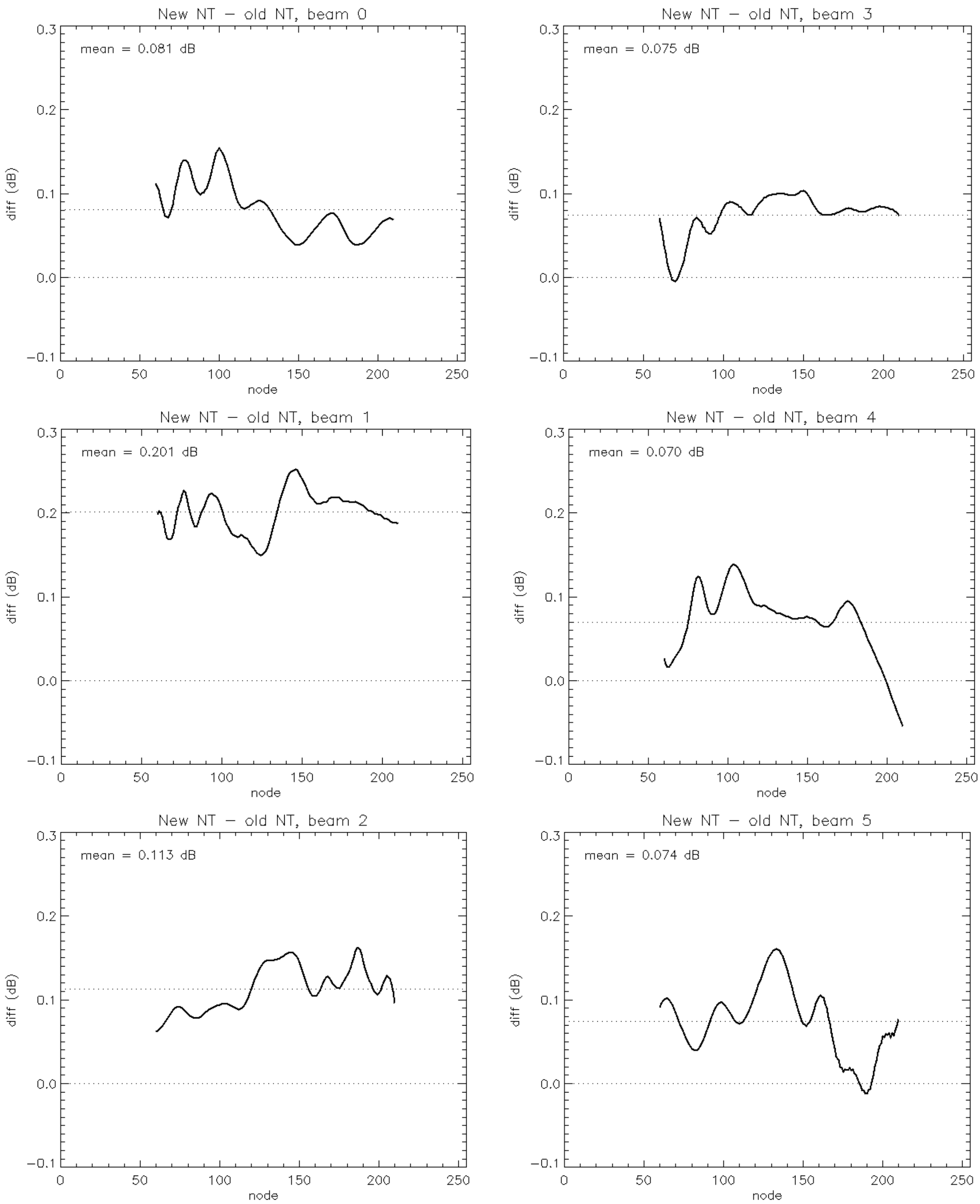

Figure 13. Difference between normalisation tables produced by the 2007 and 2010 gain patterns.

6 OCEAN BACKSCATTER

6.1 Monitoring

Ocean backscatter can be used to monitor the behaviour of the ASCAT. Figure 14 shows a section of width 0.4 dB through a three dimensional plot of ASCAT backscatter triplets from the open ocean during August 2009. The data points, shown in blue, tend to fall into two distinct regions. The black circles show the peak density of the data points in the upper region in bins of width 0.4 dB along the *x* axis. If the position of peak density is obtained for two separate months then a mean of the differences can be calculated.

Figure 15 shows the mean difference for the months of August and November 2009 as a function of incidence angle and we find that there has been a change of approximately 0.1 dB.

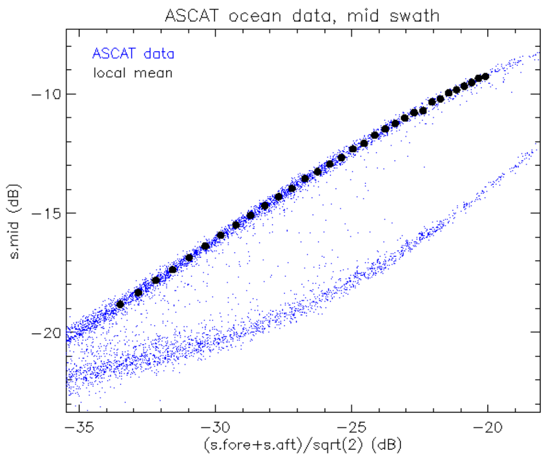

Figure 14. Section through a three dimensional plot where the x, y and z axes correspond to the fore, mid and aft backscatter from ocean σ_0 triplets. Blue points show data from the left hand beams during August 2009 and black circles show the position of the maximum density of the data points in the upper region in bins along the x axis.

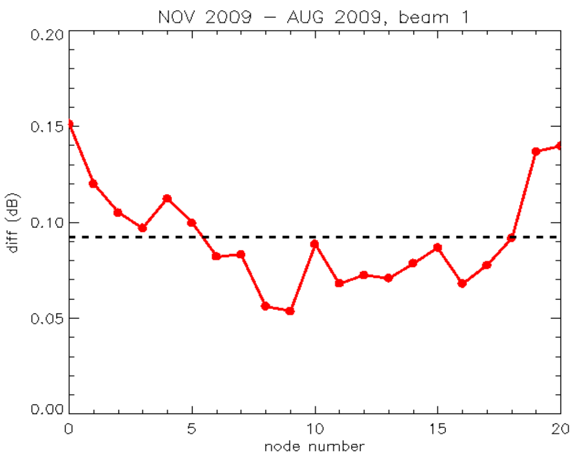

Figure 15. Mean difference between the positions of maximum density in data from August and November 2009.

This suggests that there has been a change of about 0.1 dB in the left mid beam backscatter between these dates.

This approach can also be used to determine the date on which the change took place. If we calculate the position of the peak density using data from August 2009 then the number of ocean triplets in each orbit lying above and below this position should be approximately equal and remain constant over time. However, as shown in figure 16, the number of triplets above this position increases suddenly on September 11th 2009.

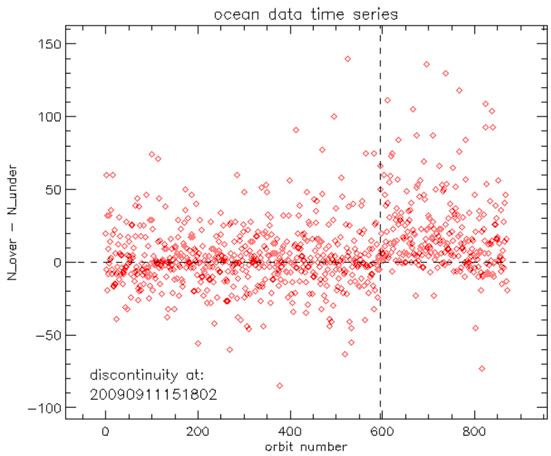

Figure 16. Difference in the number of ocean triplets above and below the position of maximum density in each orbit during August and September 2009.

6.2 Time Series

Figure 17 shows the monthly mean ocean backscatter between January 2007 and December 2010.

Beams 0 and 5 show an upward trend in backscatter, beam 1 shows no trend and beams 2, 3 and 4 show that the backscatter is decreasing over this time period.

This is inconsistent with the result of the transponder calibration which implies that the backscatter is decreasing in all beams. However it should be noted that the size of the trend in these plots is small compared to the noise in the data and hence it is not clear if these trends are statistically meaningful or reliable.

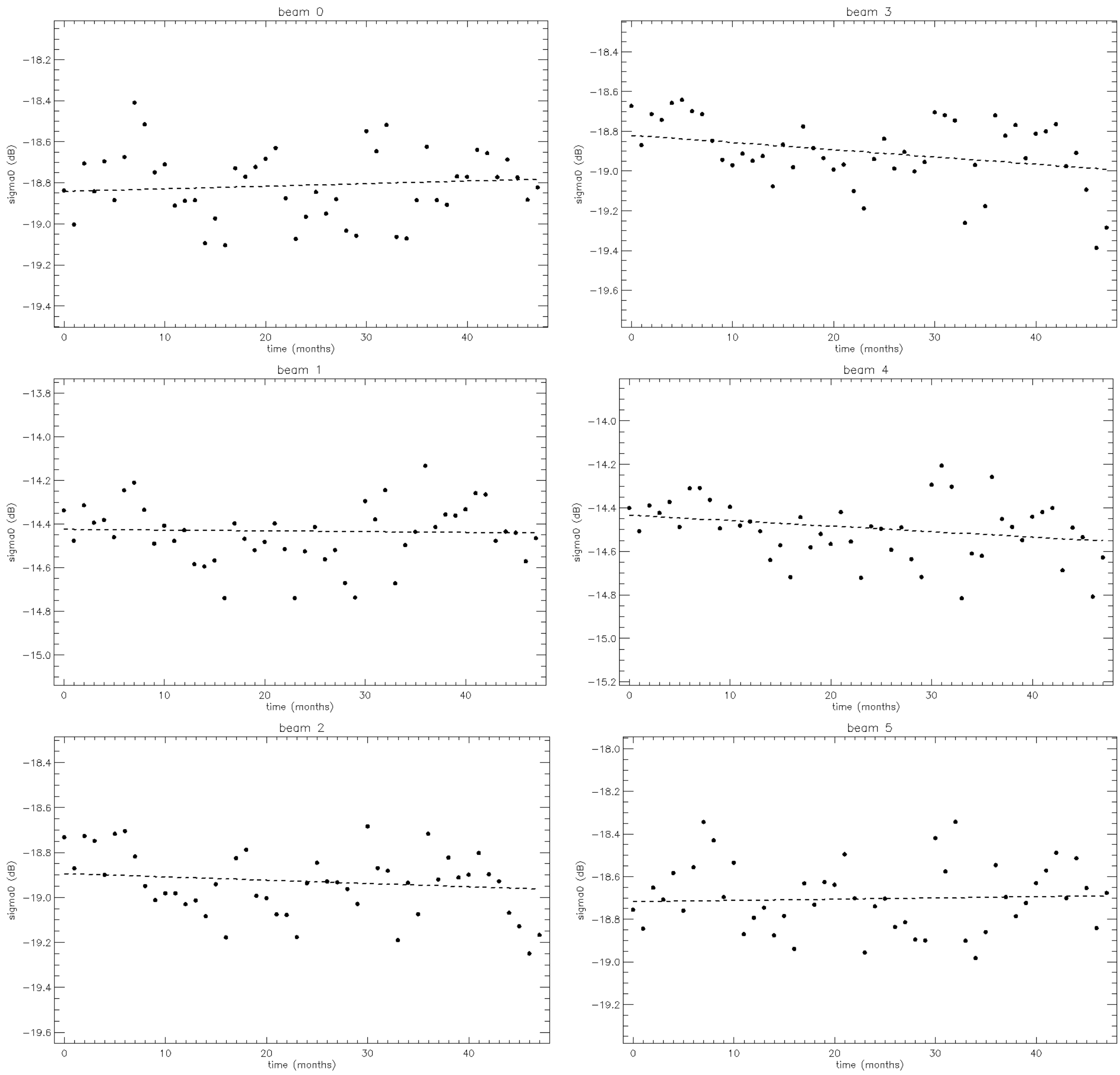

Figure 17. Monthly mean backscatter from the open ocean between ±50° latitude from January 2007 to December 2010.

The OSI-SAF validates the level 1b product by comparing the ASCAT ocean backscatter against a model backscatter produced from CMOD-5 and ECMWF wind vectors and the results are reported in [5]. Figure 18 is taken from this report and shows the mean difference between ASCAT and model backscatter over a three year period.

This plot shows a downward trend of about 0.1 dB. This may be caused by either a gradual decrease in ASCAT backscatter or an increase in the ECMWF wind speeds away from the actual real ocean wind speed.

As OSI-SAF comparisons of ECMWF wind against buoy measurements suggests that they are correct this implies a decrease in ASCAT backscatter which is inconsistent with the results from the transponders.

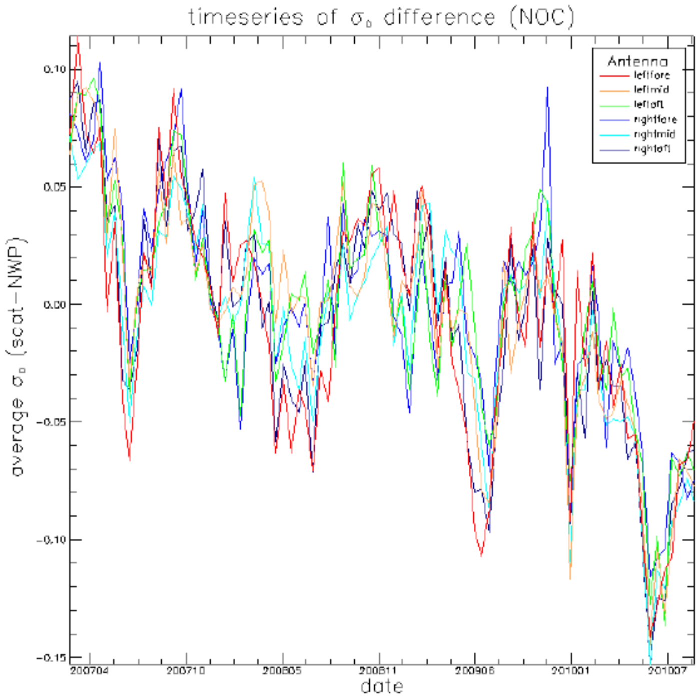

Figure 18. Time series of ASCAT NWP tocean calibration residuals for each antenna taken from [5]. NOC corrections have been applied and 0.125 dB has been subtracted from the left mid beam backscatter from September 2009 onwards.

7 RAINFOREST BACKSCATTER

Table 14 shows the change in gain between the two calibrations as taken from table 12. Also shown is the approximate change expected in backscatter, given by multiplying the change in gain by a factor of two and inverting the sign. We see that the update of the calibration to reflect the new results is expected to reduce the backscatter by approximately 0.2 dB in beam 1 and 0.1 dB in the other beams.

beam	Δ gain	$\Delta\ \sigma_0$
0	0.039	-0.078
1	0.098	-0.196
2	0.056	-0.112
3	0.035	-0.070
4	0.032	-0.064
5	0.041	-0.082

Table 14. Change in gain between the calibrations and the approximate corresponding change expected in backscatter.

If this corrects for changes in the ASCAT instrument, we would then expect to observe that the backscatter produced from ASCAT measurements in the period between the two calibration campaigns would have increased by approximately 0.2 dB in beam 1 and 0.1 dB in the other beams.

In this section we examine several years of backscatter data from an area of Amazon rainforest to determine if it has behaved in this manner, in order to gain confidence in the assumption that the changes in gain that we see from transponder measurements, as explained in the previous sections, can be explained by changes in the instrument.

Figures 19 and 20 show the mean rainforest γ_0 as a function of incidence angle for ascending and descending passes during the periods

- September 2007 – August 2008,
- September 2007 – August 2009,
- September 2009 – August 2010.

These periods were chosen to avoid averaging over the sudden step change in beam 1 (which as shown in the previous section happened in September 2009). Full-year data periods are further chosen to try to avoid rainforest seasonal variations affecting the comparison.

The legend in the plots also show the mean value of γ_0 over the entire incidence angle range for the different time periods and from this information the change in γ_0 between the first and last periods can be readily be calculated and is shown in table 15. The values as estimated from ascending and descending values are consistent and the average change is given then for all passes in the last column.

beam	ascending	descending	average
0	-0.018	-0.007	-0.012

1	0.081	0.079	0.080
2	-0.016	-0.010	-0.013
3	-0.020	-0.010	-0.015
4	-0.032	-0.031	-0.031
5	-0.019	-0.014	-0.016

Table 15. Change in mean rainforest γ_0 (in dB).

These values do not agree with the expected change shown in the last column of table 14. However, the rainforest is not a static target and its backscatter also varies over time. If, for example, the mean rainforest γ_0 in beam 4 has decreased by 0.095 dB due to variations in local climate as well as increasing by 0.064 dB due to changes in ASCAT then we obtain the observed value of -0.031 dB. Table 16 shows the rainforest behaviour required in order to bring the observed changes in rainforest into alignment with the transponder results.

beam	average
0	0.090
1	0.116
2	0.125
3	0.085
4	0.095
5	0.098

Table 16. Change in mean rainforest γ_0 (in dB) required to bring the observed figures into agreement with the results from the calibration analysis.

If we assume the rainforest is isotropic then we would expect the change in all beams to be similar. The figures in figure 16 show that this is approximately the case and hence we can conclude that the rainforest results are consistent with the transponders.

However, we note that

- the figures in table 14 show that the effect on the backscatter from ASCAT gain changes are around 0.1 dB in all beams (excluding beam 1), and that
- the figures in table 15 indicate that rainforest backscatter is essentially stable to around 0.015 dB (excluding beam 1).

Hence the above analysis is essentially assuming that there is a local change in rainforest backscatter that cancels out the effects of the changes in ASCAT gain in order to keep the backscatter from the rainforest constant. If the transponders had suggested a gain change of 1.1 dB in each beam then the stable rainforest backscatter could be explained by assuming a local rainforest change of -1.1 dB.

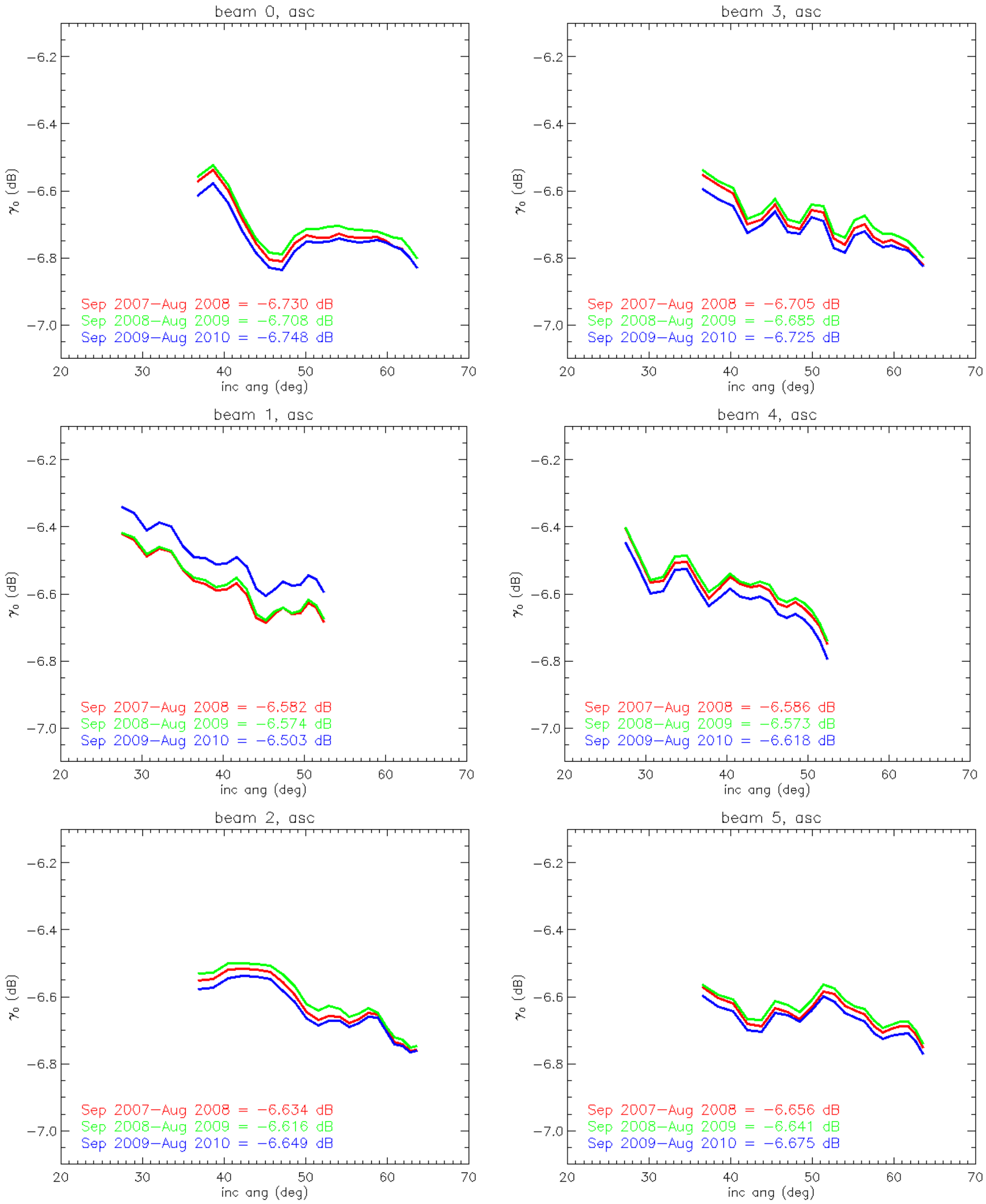

Figure 19. Rainforest γ_0 in ascending passes.

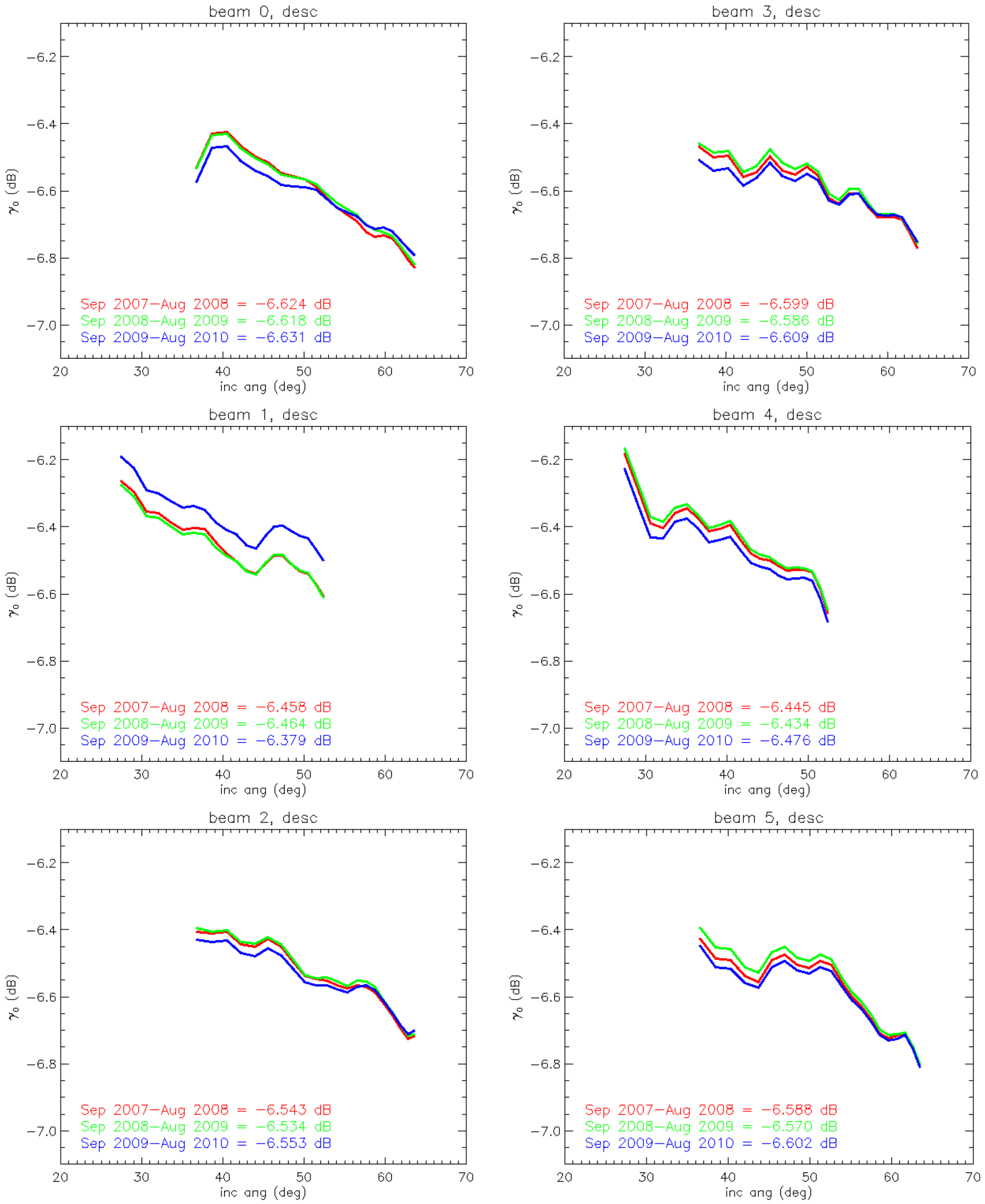

Figure 20. Rainforest γ_0 in descending passes.

We can also examine several different rainforest areas in order to identify common trends in the backscatter and hence remove or reduce localised effects. Figure 21 shows three regions of stable backscatter in the Amazon, central Africa and Borneo that were located by looking for areas where the standard deviation in the backscatter in each beam, at each incidence angle and in each of four years was less than ±0.25 dB. Note that the region in Borneo is relatively small compared to the other two.

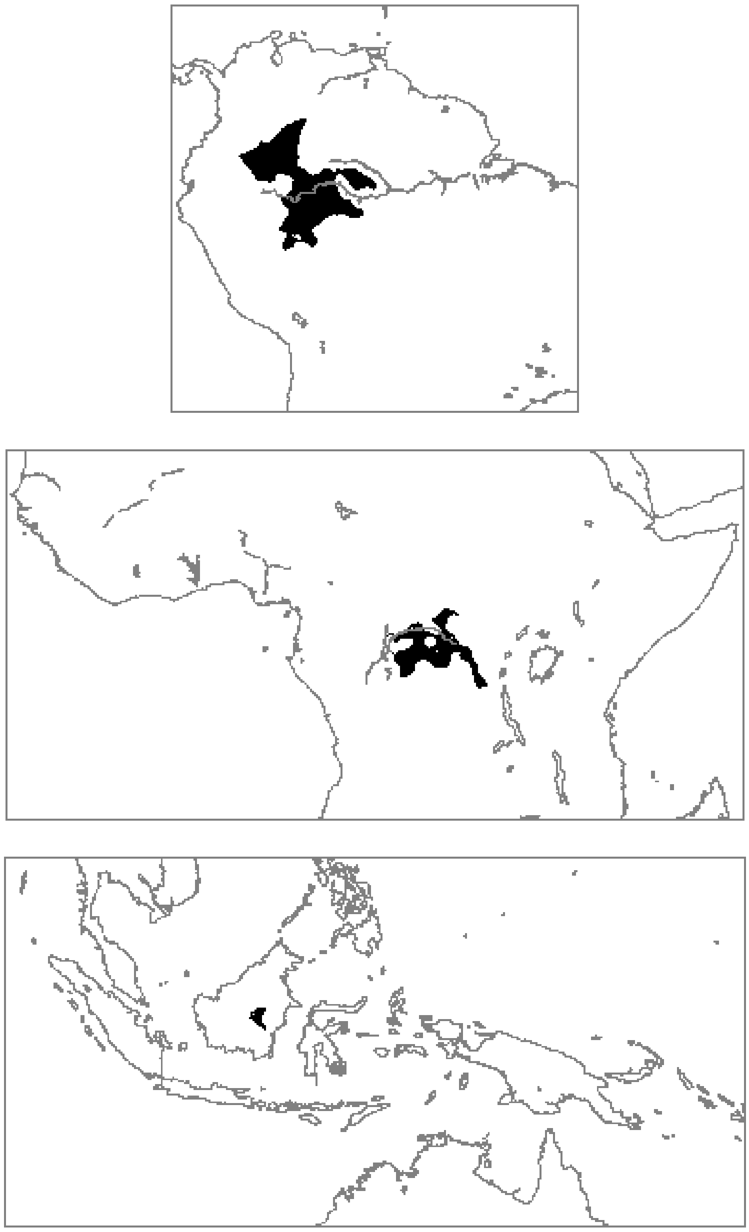

Figure 21. Maps showing areas of stable backscatter in the Amazon, central Africa and Borneo.

The behaviour of the mean γ_0 in these regions is shown in figure 22 for each beam and for ascending and descending passes. Beam 1 shows an upward trend for all regions beginning in 2009 which can be explained by the sudden change in the left mid antenna that took place in September 2009. The mean γ_0 in other beams seems to be approximately constant for all of the regions hence there is no evidence for the increase of 0.1 dB which the analysis of the transponder data implies took place over this period.

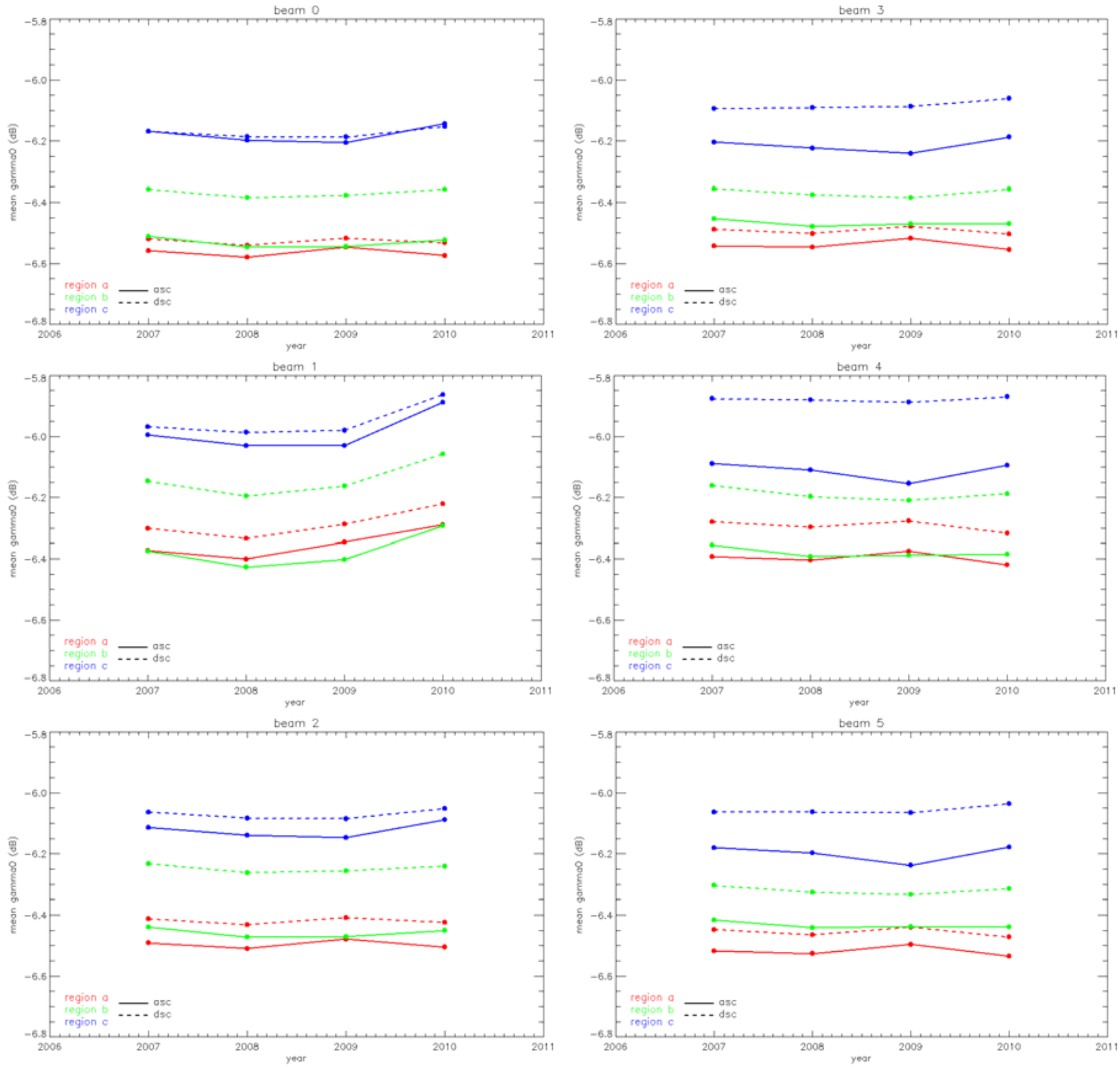

Figure 22. Annual mean γ_0 in the Amazon, central Africa and Borneo regions over a four year period.

This is confirmed in table 17 which shows the change in mean γ_0 between 2007 and 2009 in all beams. Although this varies between the three sites, it is similar in each beam and of the order of a few hundredth of a dB. As before, we could always assume some kind of local change in these three regions which cancels out the 0.1 dB change implied by the transponder analysis to give these results.

beam	Amazon	Africa	Borneo
0	0.01	-0.03	-0.03
1	0.02	-0.02	-0.02
2	0.01	-0.02	-0.03
3	0.02	-0.03	-0.01
4	0.01	-0.04	-0.04
5	0.01	-0.03	-0.03

Table 17. Change in mean backscatter (in dB) between 2007 and 2009.

8 OSCILLATIONS

As discussed in section 4, the gain patterns produced from the 2007 data using the original AGPO algorithm contain oscillations. In this section we investigate the gain patterns produced from the 2010 data with the modified AGPO algorithms to determine if the oscillations have been successfully removed.

Figure 23 shows contour plots of the original and new beam 3 gain patterns. The original clearly shows oscillations while the new pattern appears much smoother.

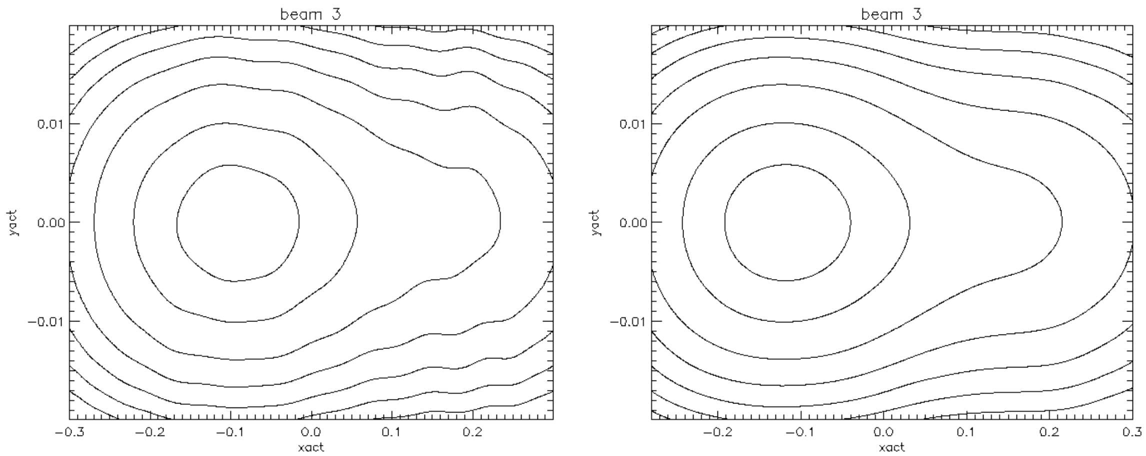

Figure 23. Contour plots of the original and new beam 3 gain patterns.

Figure 24 shows cuts through these gain patterns towards the edge of the beam. The original pattern, shown in red, clearly shows a number of oscillations while the new pattern, shown in green, is much smoother.

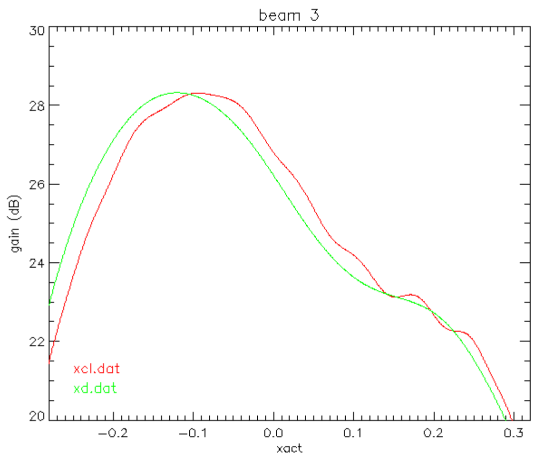

Figure 24. Gain along cuts through the edge of the original and new beam 3 gain patterns.

To examine the oscillations in more detail we plot the difference between a smoothed and non-smoothed gain pattern. Figure 25 shows the results and we can clearly see that the original gain pattern contains many oscillations whereas the new pattern is virtually oscillation free.

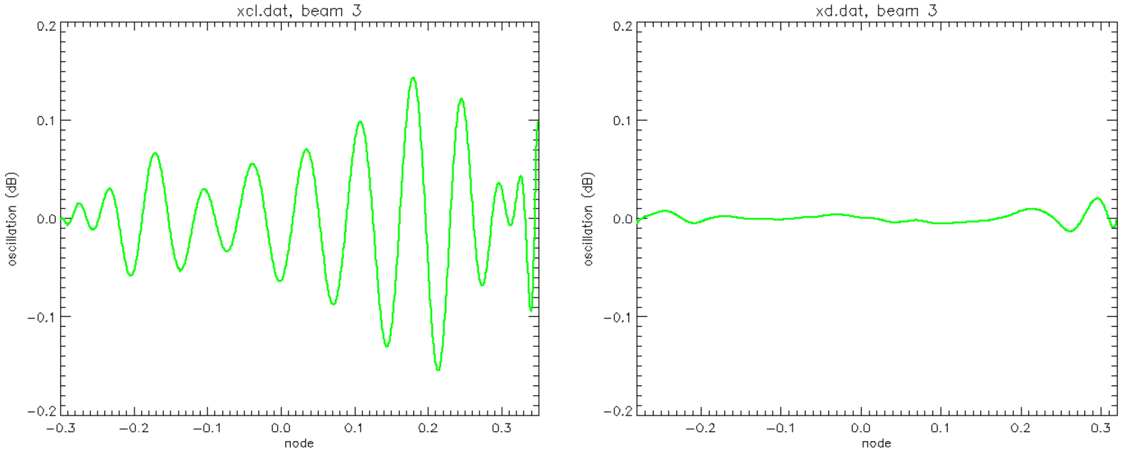

Figure 25. Oscillations in the original and new beam 3 gain patterns.

This method for highlighting oscillations can also be applied to the normalisation tables produced from the gain patterns. Figure 26 shows the difference between smoothed and non-smoothed normalisation tables produced from the original and new gain patterns. The new normalisation table clearly shows much less oscillations than the original.

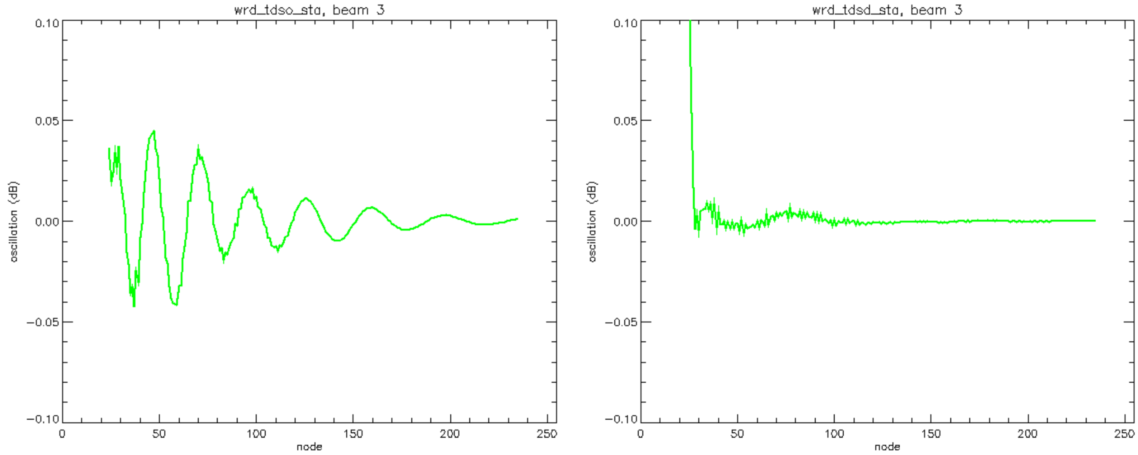

Figure 26. Oscillations in the normalization tables derived from the original and new beam 3 gain patterns.

These plots give confidence that the new AGPO algorithms have solved the oscillation problem. However, a detailed examination of backscatter produced using the new calibration is necessary to confirm this.

9 SEASONAL EFFECTS

The analysis of the calibration data given in earlier sections shows that the antenna gain as measured by the transponders is around 0.04 dB larger in 2010 than it was in 2007. As the 2007 calibration campaign took place in winter while the 2010 campaign took place in summer it is possible that different atmospheric conditions are responsible for this increase.

Figure 27 (obtained from http://www.climatetemp.info) shows the typical climate conditions in Ankara in Turkey. The relative humidity in winter is around 80% and drops to around 40% in summer. If the microwave attenuation varies with the humidity then we would expect less attenuation in summer and hence a larger signal from the transponders.

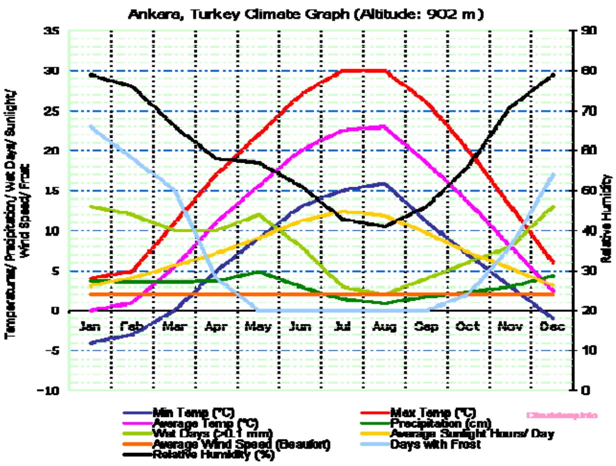

Figure 27. Climate information for Ankara, Turkey.

A model is presented in [1] in which the atmospheric attenuation of microwaves is a function of the surface temperature, pressure and relative humidity.

A graph of the attenuation given by the model is also presented which indicates that the attenuation at 5 GHz and 25% relative humidity is 0.002 dB/km. At the attenuation in the model is a linear function of the relative humidity we can use this information to estimate the seasonal effects. If the vertical scale length of the water vapour in the atmosphere is taken to be 2 km, then a viewing geometry of 45 degrees gives a scale length of 3 km. Multiplying this by 0.002 dB/km gives total loss of 0.006 dB and dividing by 25 gives a 0.0003 dB loss per percentage point of relative humidity. With 40% relative humidity in summer the loss will be therefore be 0.01 dB and with 80% relative humidity in winter the loss is 0.02 dB. The transponder signal will be therefore be 0.01 dB higher in summer than in winter which is not large enough to explain the observed increase.

Quantitative results from the model are shown in table 18 for two different relative humidities. Multiplying these by a scale height of 3 km gives summer and winter losses of 0.009 dB and 0.018 dB and hence a difference of 0.009 dB. This agrees with the earlier estimate of 0.01 dB.

Input parameters	Attenuation (dB/km)
temperature = 300 K pressure = 1013 mbar relative humidity = 80%	0.00626
temperature = 300 K pressure = 1013 mbar relative humidity = 40%	0.00298

Table 18. Model Attenuation for different summer and winter humidities.

Table 19 shows model results with typical summer and winter temperatures and relative humidities. Multiplying these by a scale height of 3 km gives summer and winter losses of 0.004 dB and 0.009 dB and hence a difference of 0.005 dB which is now smaller than before. Some evidence is presented in [4] to suggest that the scale height is smaller in winter than in summer. Taking the summer and winter vertical scale heights to be 2.85 and 1.14 km leads to attenuations of 0.002 and 0.013 dB and hence a difference of 0.011 dB.

Input parameters	Attenuation (dB/km)
temperature = 273 K pressure = 1013 mbar relative humidity = 80%	0.00126
temperature = 300 K pressure = 1013 mbar relative humidity = 40%	0.00298

Table 19. Model Attenuation for different summer and winter temperatures and humidities.

The results from this model therefore suggest that the different atmospheric conditions in summer compared to winter can increase the signal by around 0.01 dB. This is not large enough to explain the observed increase of approximately 0.04 dB

10 CONCLUSIONS & RECOMMENDATIONS

The ASCAT calibration algorithms have been modified to deal with differences in the azimuthal pointing between ascending and descending passes that give oscillations in the gain patterns. The updated algorithms have been used to process data from the summer 2010 campaign and data from the previous winter 2007 campaign. Examination of the results shows that the oscillations have been successfully removed. Comparison of the two sets of gain patterns derived from the transponder data shows that the gain has increased by approximately 0.1 dB in beam 1 and 0.04 dB in the other beams over this time period. This implies that the estimate of backscatter produced by the ASCAT processor during this time period has increased by 0.2 dB in beam 1 and approximately 0.08 dB in the other beams.

The increases in gain are larger than the RMS error in the gain pattern and are therefore statistically significant. However, the gain increase may either be a result of changes in the ASCAT or due to some kind of systematic effect related to the transponders. Systematic effects due to differences in ambient temperature between the summer and winter calibrations can be discounted as the transponder electronics are temperature controlled. A model of microwave attenuation due to atmospheric water vapour has been investigated and indicates that the difference in humidity between summer and winter may give rise to an increase in gain of approximately 0.01 dB. This is much less than the observed values and hence it seems likely that the observed increase in gain reflects real changes in the ASCAT gain patterns.

ASCAT data over the open ocean during 2009 has been investigated and shows that the backscatter in beam 1 changed suddenly by about 0.1 dB on the 11th of September 2009. The magnitude of this change is consistent with the results of the gain pattern analysis.

Time series of rainforest backscatter, ocean backscatter and ocean validation residuals have been examined to determine if they are consistent with the increase in backscatter values predicted from the calibration analysis. We find that:

- The rainforest data shows that (with the exception of beam 1) the backscatter is generally stable with any changes much smaller than those predicted. However, these results are consistent if there had been an environmental change that decreased the rainforest backscatter by about 0.1 dB (which would then combine with the approximately 0.1 dB increase due to changes in the gain pattern to give the observed stability).

- The time series of mean ocean backscatter show different trends in different beams and over different time periods. However as the observed trend is small compared to the noise in the data it is not clear that these results are significant.

- The ocean validation performed by the OSI-SAF, which examines the residual between ASCAT backscatter and a model backscatter given by CMOD5 and ECMWF winds, has found a trend consistent either with decreasing ASCAT backscatter or increasing ECMWF wind speed. As the ECMWF winds appear to be consistent with buoy measurements then the implication is that ASCAT backscatter is decreasing over time.

The analysis presented in this document indicates that the gain pattern and normalisation tables from the new algorithms have an improved quality (with respect to the oscillations in the beam pattern) and accurately correct changes to the left mid beam that took place in September 2009. However the predicted increase in the estimated backscatter has not been confirmed by analysis of rainforest backscatter, ocean backscatter or by ocean validation. We note however that these analyses are not straightforward and may be affected by a variety of other factors.

As there is no reason to believe that there are any errors in the results produced by the 2010 calibration campaign, it is recommended that the new calibration tables are introduced into the ASCAT processor in order to correct the changes in beam 1 and to reduce oscillations in the backscatter.

It is further recommended that

- EUMETSAT liaises with the users involved in the definition of geophysical retrieval models for ASCAT (winds, sea ice and soil moisture) in order to use the 2010 calibration results as a reference calibration to base the Level 2 product retrieval models.

- Frequent transponder campaigns should be regarded as a high priority in order to investigate gain pattern variability and rule out any possible systematic effects associated with the transponders.

- Geophysical analysis of ASCAT backscatter should be improved so that, if possible, time series trends can be more clearly determined in order to give confirmation of calibration results.

REFERENCES

[1] ASCAT Commissioning Quality Report, EUM.MET.REP.08.0525

[2] Wilson JJW, Anderson C *et al* (2010) “Radiometric calibration of the advanced wind scatterometer radar ASCAT carried on board the METOP-A satellite,” IEEE Trans. Geosci. & Rem. Sens, vol 48, No 8, pp 3236-3255.

[3] http://descanso.jpl.nasa.gov/Monograph/series10/06_Reid_chapt+6.pdf p262/263

[4] Holdaway MA et al (1996) “Correlation between opacity and surface water vapour pressure” http://www.alma.nrao.edu/memos/html-memos/alma158/memo158.html

[5] Verspeek J, Verhoef A & Stoffelen A. (2011) “ASCAT NWP ocean calibration” OSI-SAF.

[6] Rostan F & Koch P “ASCAT transponder specification” Astrium GmbH, MO-RS-DOR-SC-0013.